

The Solar Surface Dynamo

J. Pietarila Graham,¹ S. Danilovic,¹ M. Schüssler,¹
A. Vögler,²

¹Max-Planck-Institut für Sonnensystemforschung
²Sterrekundig Instituut, Utrecht University

2nd *Hinode* Science Meeting 30.09.08

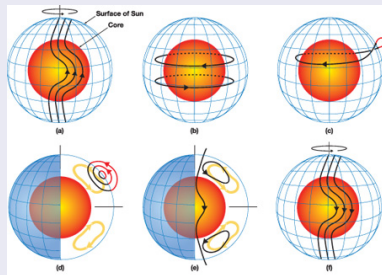
Outline

- 1 Overview of turbulent dynamo theory
- 2 Is there a small-scale solar surface dynamo (SSSD)?
- 3 MURaM solar surface dynamo

Solar global dynamo

Global dynamo

- 22 year cycle
- \approx dipolar
- many models
(Babcock-Leighton,
flux-transport (Dikpati et al.),
surface shear (Brandenburg
2005))



M. Dikpati, NCAR

Solar surface dynamo – turbulent (small-scale) dynamo?

Turbulent dynamo

- Stretching of B-field lines by turbulence (Batchelor 1950, Moffat 1978, Parker 1979)
- “Fast” dynamo for chaotic & sufficiently complex flows (Childress & Gilbert 1995)
- Near the surface layer of the sun? (e.g., Petrovay & Szakaly 1993)

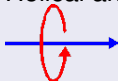
Stretching $\gg \eta$

$$\partial_t \mathbf{B} = \nabla \times (\mathbf{v} \times \mathbf{B}) + \eta \nabla^2 \mathbf{B}$$
$$Re_M = \frac{v_0 l_0}{\eta} > Re_M^C \rightarrow \text{dynamo}$$

Turbulent dynamos – well studied

Turbulent dynamos first demonstrated 20 years ago

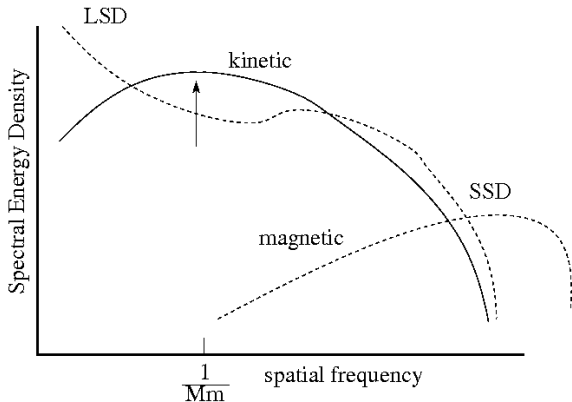
- Realistic: Boussinesq, rotation, convection in spherical shell (Gilman and Miller 1981)
- Idealistic: periodic box
 $N^3 = 64^3$, $Re_M \approx 100$ (Meneguzzi et al. 1981)
 - Homogeneity and isotropy recovered at small scales
 - Helical and Non-helical



Turbulent dynamos – large & small

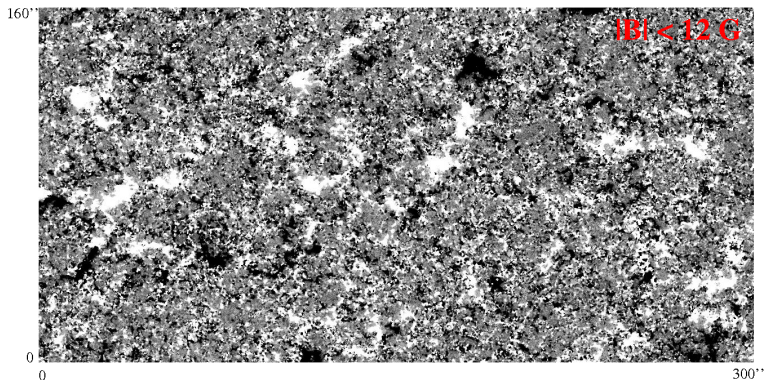
2 types of turbulent dynamos

- Large-scale (LSD; helicity, α -effect: mean-field)
- **Small-scale (SSD; non-helical)**
- solar surface dynamo
($\tau_{conv} \sim 10$ min
 $\ll \tau_{rotation}$
 \rightarrow no net helicity)



Magnetic carpet (Title and Schrijver 1998; Title 2000)

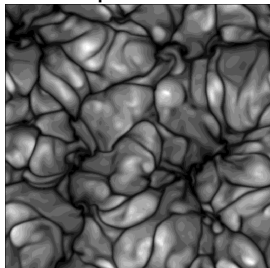
Lites et al. 2008



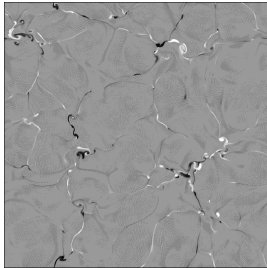
(see also Hagenaar et al. 2003)

Convectively-Driven Small-Scale Dynamo (Cattaneo 1999)

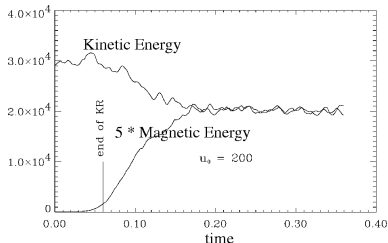
Temperature



B_z



$$Re \approx 200$$
$$Re_M \approx 1000$$
$$512 \times 512 \times 97 \approx 5 \cdot Re_M^{9/4}$$



- Boussinesq convection
- no Coriolis force (SSD)

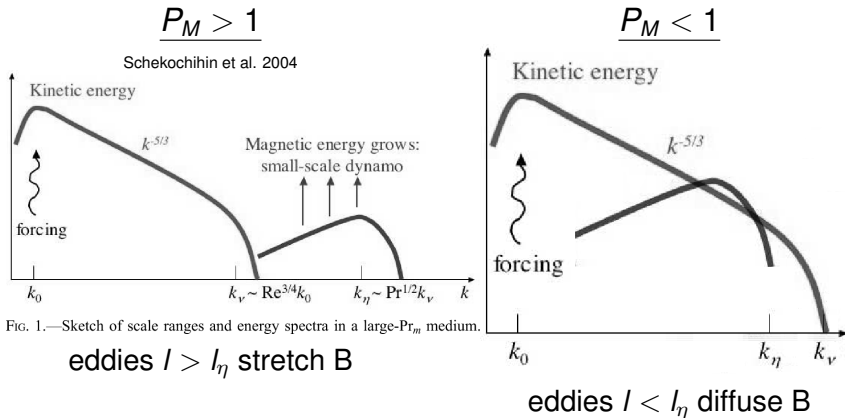
(see also Cattaneo et al. 2003)

1. Shredding of large-scale field by turbulence?

Induced small-scale field

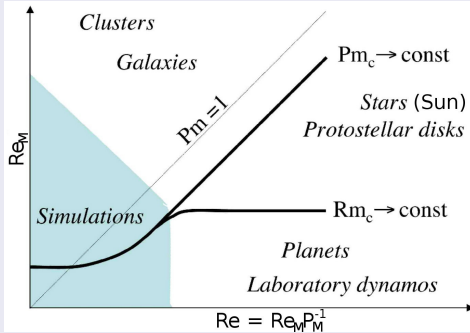
- Timescale for SSD much faster (e.g., Kulsrud & Anderson 1992; Kulsrud 1999)
 - $\tau_{SSD} \sim 10 \text{ min}$ (theoretically) \ll other dynamos
- Shredding is algebraic-in-time, SSD is exponential-in-time
(e.g., Schekochihin et al. 2005)
- **Observation:** Very small-scale bipolar regions ($\Phi < 30 \cdot 10^{18} \text{ Mx}$) independent of the solar cycle and latitude (for low latitudes) (Hagenaar et al. 2003)

2. $Re \gg Re_M$ (i.e., $P_M \equiv \frac{Re_M}{Re} = \frac{\nu}{\eta} \ll 1$)



2. $Re \gg Re_M$ (i.e., $P_M \equiv \frac{Re_M}{Re} = \frac{\nu}{\eta} \ll 1$)

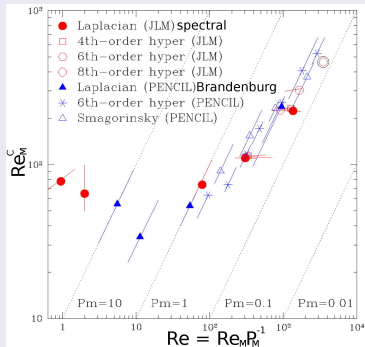
2 Theoretical possibilities



Schekochihin et al. 2005

2. $Re \gg Re_M$ (i.e., $P_M \equiv \frac{Re_M}{Re} = \frac{\nu}{\eta} \ll 1$)

No dynamo at low P_M



Schekochihin et al. 2005

Dynamo at low P_M

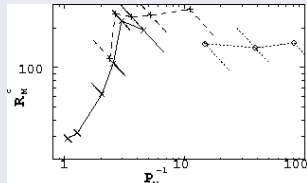
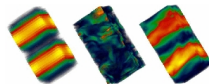
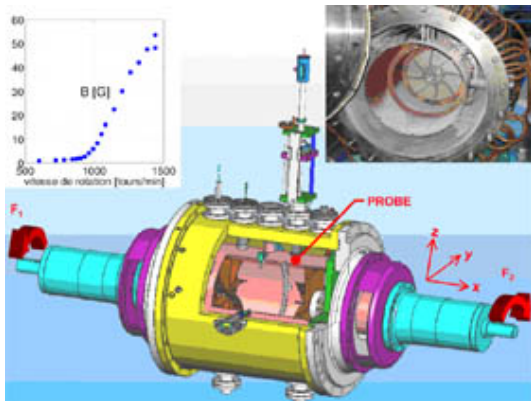


FIG. 1: Re_M^c for dynamo action versus inverse P_M . Symbols are: \times (DNS), $+$ (LAMHD), and \circ (LES). Transverse lines indicate error bars in the determination of Re_M^c , as the distance between growing and decaying runs at a constant Re .

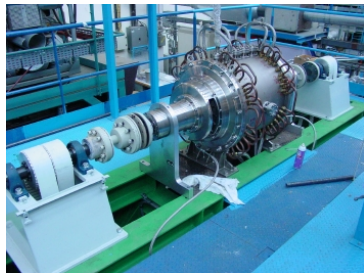
Ponty et al. 2005



$P_M \approx 10^{-5}$ – No Problem



VKS experiment (Monchaux et al. 2007)



CEA-Saclay – CNRS –
ENS-Lyon – ENS-Paris



3. Strong stratification & little recirculation

“Last” argument against SSD (Stein et al. 2003)

- Strong stratification
- Little plasma is recirculated in the near-surface layers
- Realistic magneto-convection with open boundaries (Stein et al. 2003): $253 \times 253 \times 163 \rightarrow Re_M \sim 600$

The MURaM code (Vögler et al. 2005; Vögler 2003)

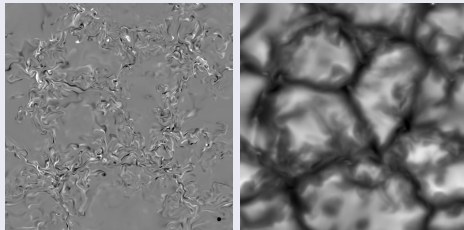
Realistic magnetoconvection

- Strong stratification
- Fully compressible
- Partial ionization
- Radiative transfer
- Open lower boundary

(vertical upflows, $\frac{dz}{dt} = 0$ for downflows; B_{hor} not advected
into box)

- No rotation
- Parallelized

B_z & brightness

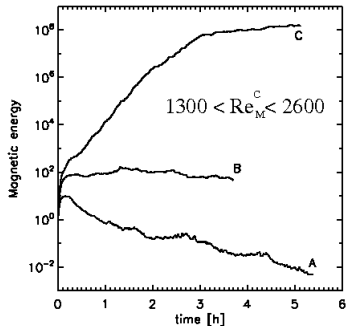


Strong stratification & little recirculation – No Problem

Vögler & Schüssler 2007

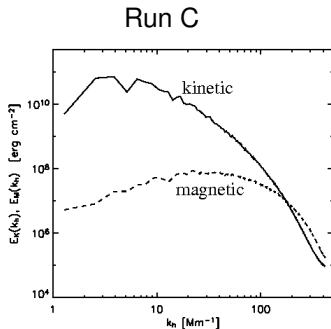
Run	$N_{hor}^2 \times N_Z$	Re_M
A	$288^2 \times 100$	300
B	$576^2 \times 100$	1300
C	$648^2 \times 140$	2600

$$1300 \lesssim Re_M^C < 2600$$



Run C: $E_M \approx 3\% E_K$

Turbulent small-scale solar surface dynamo for $Re_M > Re_M^C$



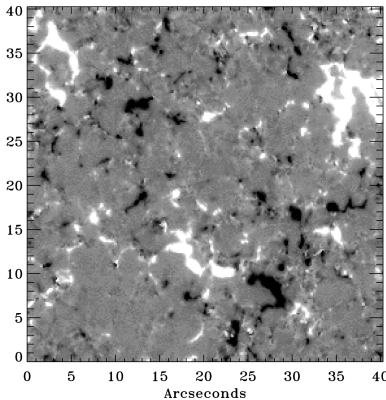
(Vögler & Schüssler 2007)

Simulation Comparison

Result	Grid pts.	Re_M	P_M	BC	SSD
Run A	$288^2 \times 100$	≈ 300	≈ 1	open	N
Stein+	$253^2 \times 163$	≈ 600	≈ 1	open	N
Run B	$576^2 \times 100$	≈ 1300	≈ 1	open	N
Cattaneo	$512^2 \times 97$	≈ 1000	≈ 5	closed	Y
Run C	$648^2 \times 140$	≈ 2600	≈ 1	open	Y

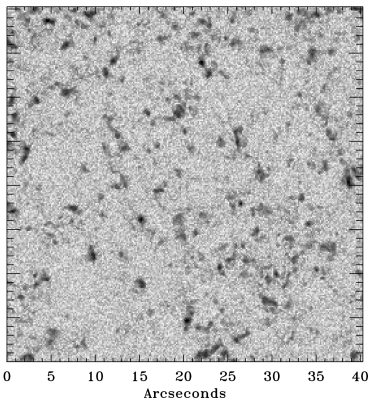
Pervasive horizontal magnetic flux (Lites et al. 2008)

$$\langle |B_{app}^L| \rangle \approx 11 \text{ Mx cm}^{-2}$$



$$|B_{app}^L| \leq 50 \text{ Mx cm}^{-2}$$

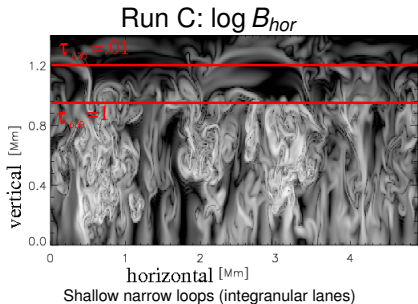
$$\langle B_{app}^T \rangle \approx 55 \text{ Mx cm}^{-2}$$



$$B_{app}^T \leq 200 \text{ Mx cm}^{-2}$$

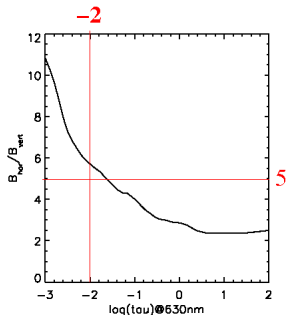
Strong horizontal photospheric magnetic field in SSD

(Schüssler & Vögler 2008)



Extended loops (above granules)

(see also Steiner et al. 2008)

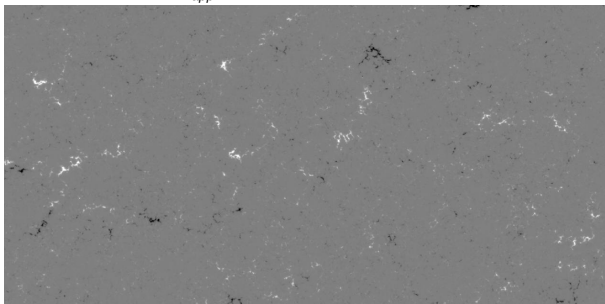


Average vertical field decreases faster with height than

horizontal field

Distribution of vertical field strength

Hinode B_{app}^L 220 Mm \times 110 Mm (Lites et al. 2008)

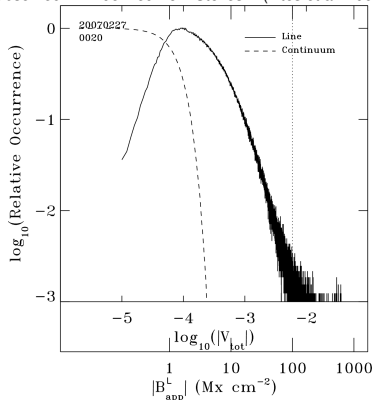


Run C: B_{ave} 4.9 Mm \times 4.9 Mm

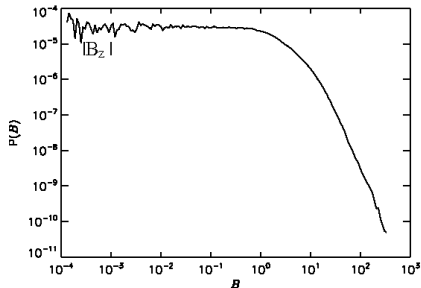


Prevalent weak vertical field

Observed PDF derived from Stokes V (Lites et al. 2008)



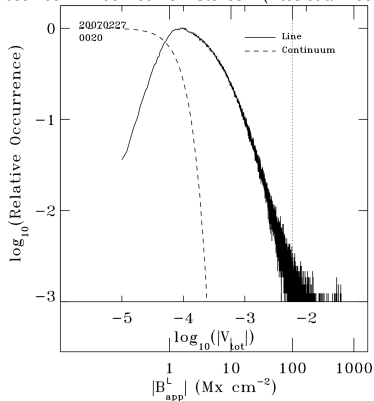
Simulated PDFs



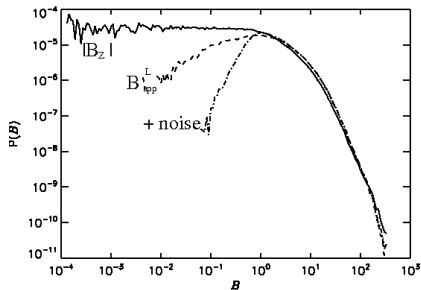
Simulations have prevalent weak field

Prevalent weak vertical field

Observed PDF derived from Stokes V (Lites et al. 2008)

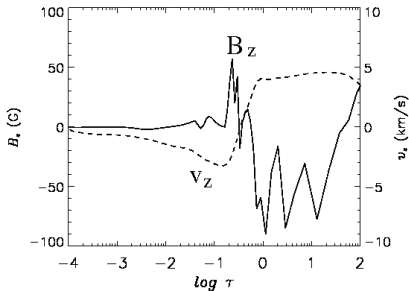


Simulated PDFs

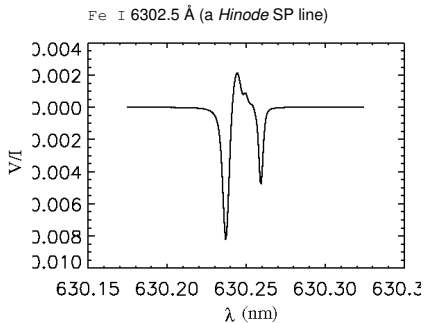


Synthetic observation is also peaked

Vertical radiative transfer & turbulence



Vertically averaged field = 0

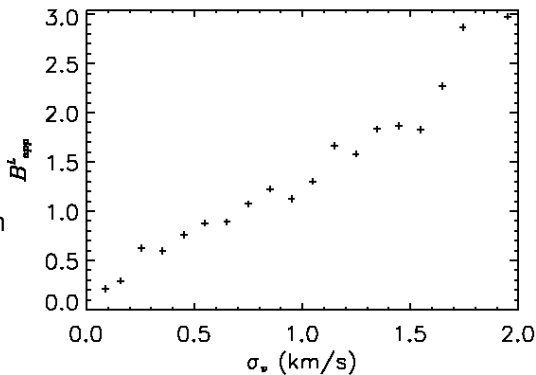


Absorption profiles Doppler shifted

Vertical radiative transfer & turbulence

$B_{ave} < 0.1 \text{ G}$

Synthetic
Magnetogram

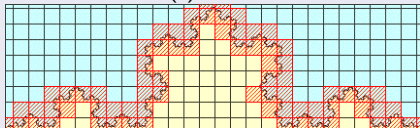


Effect increases with variance(v_z)^{1/2} along line of sight

From fractal geometry to true unsigned vertical flux

Fractal = self-similar = power-law

$$N(l) \propto l^{-D}$$



Koch fractal

$$\chi(l) \equiv \frac{\sum_i \int_{\mathcal{A}_i(l)} \mathbf{B}_z \, da}{\int_{\mathcal{A}} |\mathbf{B}_z| \, da}$$

$$\chi(l) \sim l^{-\kappa}$$

(Ott et al. 1992)

(Sorriso-Valvo et al. 2002)

Phys. Plasmas, Vol. 9, No. 1, January 2002

Analysis of oscillations in two-dimensional...

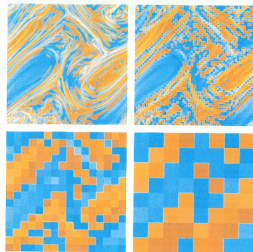
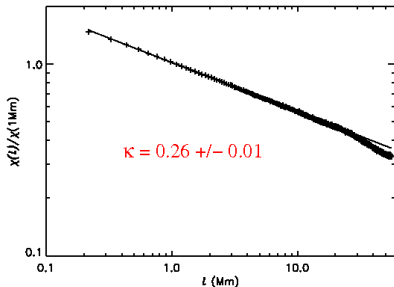


FIG. 3. 3.3015 The unsigned speed versus the vector l at $\text{tau} = 1.2$ for the 48000 box case, mesh 0.1×0.08 , 0.1×0.08 , 0.1×0.1 , 0.15×0.1 in xy plane. Green curve (left axis) for region l refers to yellow for second axis, gray curve for red axis. Circles (left axis) refer to squares for the second axis, gray curve for red axis.

$\chi(l)$ measures the portion of flux remaining after averaging over boxes of length l

Cancellation is self-similar

Hinode B_{app}^L (Lites et al. 2008)



$$\chi(l) \equiv \frac{\sum_i \left| \int_{\mathcal{A}_i(l)} \mathbf{B}_z \, da \right|}{\int_{\mathcal{A}} |\mathbf{B}_z| \, da}$$

Fractal extrapolation

$$\langle |\mathbf{B}_z| \rangle \equiv \int_{\mathcal{A}} |\mathbf{B}_z| \, da / \int_{\mathcal{A}} da$$

$$\langle |\mathbf{B}_z| \rangle_i \equiv \frac{\sum_i \left| \int_{\mathcal{A}_i(l)} \mathbf{B}_z \, da \right|}{\int_{\mathcal{A}} da} = \chi(l) \cdot \langle \mathbf{B}_z \rangle$$

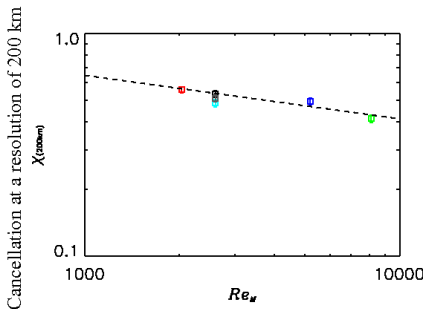
$$\langle |\mathbf{B}_z| \rangle = \langle |\mathbf{B}_z| \rangle_i \cdot \frac{\chi(l_\eta)}{\chi(l)} = 12\text{G} \cdot \left(\frac{100\text{km}}{l_\eta} \right)^{0.26}$$

$$\eta \sim 10^8 \text{ cm}^2 \text{ s}^{-1} \quad (\text{Kovitya \& Cram 1983})$$

$$\text{K41} \rightarrow l_\eta \approx 80 \text{ m} < 800 \text{ m}$$

$$\rightarrow \langle |\mathbf{B}_z| \rangle \geq 40 \text{ G}$$

Better agreement with Hanle estimates



The flux remaining at $l = 200$ km follows a power-law scaling. Extrapolation to solar values, $Re_M \sim 3 \cdot 10^5$, yields $\chi(200\text{ km}) = 0.2$.

$$\rightarrow \langle |B_Z| \rangle \sim 50 \text{ G}$$

$$\langle |B_Z| \rangle \sim 40 \text{ or } 50 \text{ G}$$

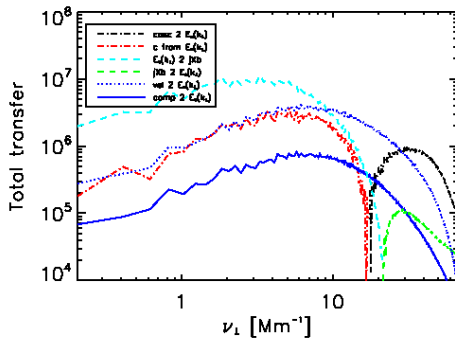
$$\langle B_{hor} \rangle \gg \langle |B_Z| \rangle \quad (\text{Lites et al. 2008})$$

$$\langle B \rangle \sim 130 \text{ G Hanle} \quad (\text{Trujillo Bueno et al. 2004})$$

Conclusions

- A small-scale solar surface dynamo (SSSD) is likely
 - Seen in *Hinode* observations
 - Dynamo simulations in agreement with observations
 - Arguments against fail: stratified, compressed, little recirculation, $P_M \ll 1$ all seem OK
- Whatever its source, small-scale B-field is turbulent & fractal
 - we should use this to interpret observations

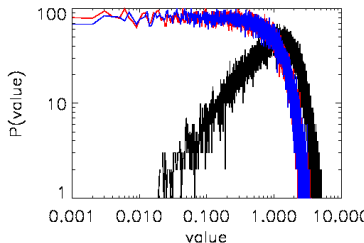
Future Work



Effect of noise

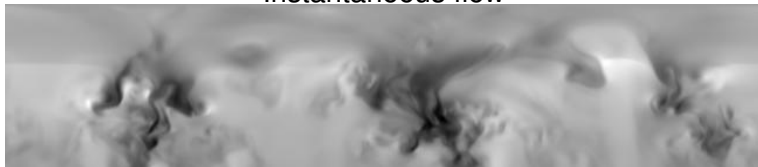
Sum of absolute values of 2 random vars

- $B_{app}^L = f(V_{tot})$
- $V_{tot} = \text{sgn}(V_{blue}) \cdot \frac{1}{l_c N} (|\sum_{i=1}^{N_b} (V(\lambda_i) + \sigma_i) \Delta \lambda| + |\sum_{i=1}^{N_r} (V(\lambda_i) + \sigma_i) \Delta \lambda|)$
- $|V_{tot}| = |V_{tot}^{true}| + \frac{1}{l_c N} (|\sigma_b| + |\sigma_r|)$
- For $|V_{tot}^{true}| \approx 0 \rightarrow |V_{tot}| > 0$
(artificially high flux)



Mean flow

Instantaneous flow



Time-averaged mean flow



Pictures of Dynamos

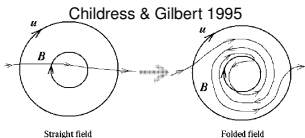
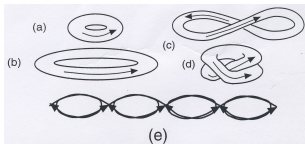
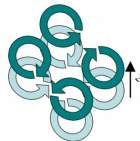
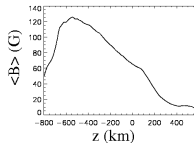


FIG. 2.—Stretching and folding of field lines by turbulent eddies.

Schekochihin et al. 2004

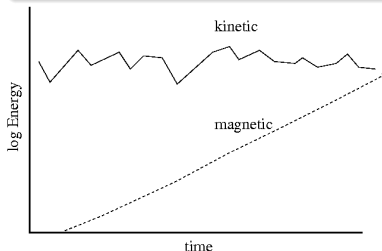
$$N^3 \propto Re_M^{9/4}$$



What is dynamo action?

1. Kinematic/exciting

- Kinematic – generates B-field from seed (non-magnetic state is unstable)



2. General/sustaining

- General – maintains B-field against losses of ohmic dissipation: $\eta \nabla^2 B$

